ELECTROMAGNETIC BACKSCATTERING OF RADIATION WAVE OF SATELLITE ANTENNA DUE TO OBJECTS ON RANDOM GROUND SURFACES

Yasumitsu MIYAZAKI, Tomonori KAWAKAMI and Koichi TAKAHASHI
Department of Information and Computer Sciences
Toyohashi University of Technology
Tempaku-cho, Toyohashi, Aichi, 441-8580 JAPAN
E-MAIL miyazaki@emlab.tutics.tut.ac.jp

1. Introduction

Repeated acquisition of data of earth's environment over a large area in a short period of time becomes possible using remote sensing by satellite. Because it is a sensing technology without the influence of various phenomena that occur on the surface of the earth, it has a wide application range and there has recently been increasing attention. Especially considerations towards the Geographic Information System (GIS) is given increasing importance. Recently, remarkable improvements have been made in the area of sensor loaded satellite remote sensing of earth, and rapid progress on the resolution is achieved. Although the space resolution of SAR is about 10 m when it is carried on the satellite, a resolution of about 1 m in the case of optical sensor has been obtained. An advantage of using SAR is that it is possible for stable observation independent of the season, day and night, weather, because it is an active sensor that does not utilize the solar light. The resolution of SAR is lower than that of optical sensor when microwaves are used.

In this research, the characteristics of backscattering of electromagnetic wave by random surface are analyzed as a basis to improve the resolution of the sensor that uses microwaves. And we followed a statistical analysis of scattering by random surface [1-4]. We characterized the object located on the random surface by analyzing the electromagnetic scattering of incident pulse wave using a numerical technique [5], which combines finite difference time domain (FDTD) method [6,7] and near-to-far field transformation.

Remote sensing of the ground using pulse radar is numerically analyzed using the above technique. To obtain received far field scattered signal by random surface at the satellite, we employed near-to-far field transformation.

2. Analysis of Field Model

2.1. Simulation Parameters

Numerical simulation results are presented for the case of TE polarization (Ez=0). We considered a two-dimensional simulation model as illustrated in Fig. 1. The carrier frequency f of incident pulse is assumed to be in the range of 1.5, 6, 10 GHz, and the response is analyzed in time domain of electromagnetic wave. The object shown in the model is assumed to be dielectric, ε_r=2.8 with a width and height of 10 wavelengths. Similar models have been constructed for the other frequencies used in the simulations. To simplify the problem, we assumed the ground media to be a perfect electric conductor (PEC). The antenna is assumed to be at a height of 568 km above the ground. Boundary condition for FDTD method uses Mur second order absorbing boundary condition [8].

2.2 Radiation Field Formulation

Wave equations of electromagnetic fields are

$$\left(\nabla^2 - \frac{1}{c^2}\frac{\partial^2}{\partial t^2}\right)\mathbf{E}(\mathbf{r},t) = \mu\frac{\partial \mathbf{J}(\mathbf{r},t)}{\partial t} \qquad (1)$$

$$\left(\nabla^2 - \frac{1}{c^2}\frac{\partial^2}{\partial t^2}\right)\mathbf{H}(\mathbf{r},t) = -\nabla\times\mathbf{J}(\mathbf{r},t)\cdot \qquad (2)$$

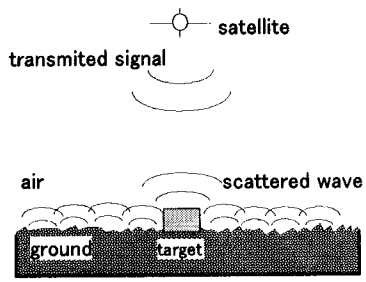

Fig.1 Schematic of satellite remote sensing.

From Eqs. (1) and (2) the two-dimensional Green's function is derived as follows:

$$G(\mathbf{r},t|\mathbf{r}',t') = \frac{1}{2\pi c}\frac{1}{\sqrt{\{c(t-t')\}^2 - |\mathbf{r}-\mathbf{r}'|^2}} \qquad t > t' + |r - r'|/c \qquad (3)$$

$$G(\mathbf{r},t|\mathbf{r}',t') = 0 \qquad t < t' + |r - r'|/c\,. \qquad (4)$$

Electric field component E_y is given by,

$$E_y(\mathbf{r},t) = -\frac{1}{2\pi c}\int_0^{t-R/c}\int_{-\infty}^{\infty} G(\mathbf{r},\mathbf{r}';t,t')\cdot\frac{\partial J_y(\mathbf{r}',t')}{\partial t'}dS'dt' \quad (5)$$

Similarly, we can derive the expressions for magnetic field components H_x and H_z, and are given by,

$$H_x(\mathbf{r},t) = -\frac{1}{2\pi c}\int_0^{t-R/c}\int_{-\infty}^{\infty} G(\mathbf{r},\mathbf{r}';t,t')\cdot\frac{\partial J_y(\mathbf{r}',t')}{\partial z}dS'dt' \quad (6)$$

$$H_z(\mathbf{r},t) = -\frac{1}{2\pi c}\int_0^{t-R/c}\int_{-\infty}^{\infty} G(\mathbf{r},\mathbf{r}';t,t')\cdot\frac{\partial J_y(\mathbf{r}',t')}{\partial x}dS'dt' \quad (7)$$

where J_y is shown in Fig. 2, which, at the position of the antenna shown in Fig. 3, is given by

$$J_y(t) = \begin{cases} \cos(2\pi f_c t) & 0 \le t \le \tau,\ x_L \le x \le x_R,\ z = z_0 \\ 0 & otherwise \end{cases} \quad (8)$$

where $x_L = x_0 - 1$ m, $x_R = x_0 - 1$ m.

2.3 Near-to-Far Field Transformation

In order to investigate the electromagnetic field scattering from the objects located on the ground surface, it is necessary to derive the electric field distribution at the location of satellite antenna, shown in Fig. 4. The equivalent electromagnetic current given by Eq. (9) on the Huygens surface is calculated from the scattered near-field derived using FDTD method, and we consider the far-field transformation of the near field for the present investigation.

$$\mathbf{J}_s = \mathbf{n}\times\mathbf{H} \quad , \quad \mathbf{M}_s = -\mathbf{n}\times\mathbf{E} \quad (9)$$

By using the two-dimensional Green's function (Eq. (3)) in the wave equations,

$$\left(\nabla^2 - \frac{1}{c^2}\frac{\partial^2}{\partial t^2}\right)\mathbf{E}(\mathbf{r},t) = \mu\frac{\partial \mathbf{Js}(\mathbf{r},t)}{\partial t} + \nabla\times\mathbf{Ms}(\mathbf{r},t) \quad (10)$$

$$\left(\nabla^2 - \frac{1}{c^2}\frac{\partial^2}{\partial t^2}\right)\mathbf{H}(\mathbf{r},t) = \varepsilon\frac{\partial \mathbf{Ms}(\mathbf{r},t)}{\partial t} - \nabla\times\mathbf{Js}(\mathbf{r},t) \quad (11)$$

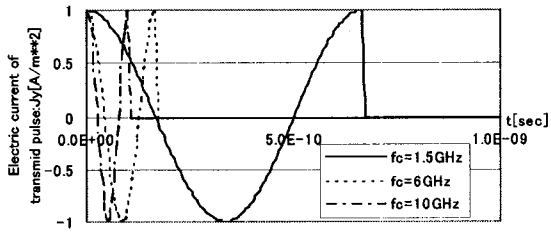

Fig. 2 Electric current of incident pulse.

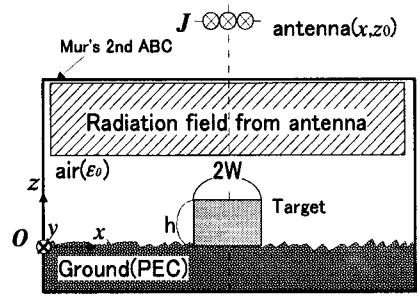

Fig. 3 Schematic of FDTD Calculation model.

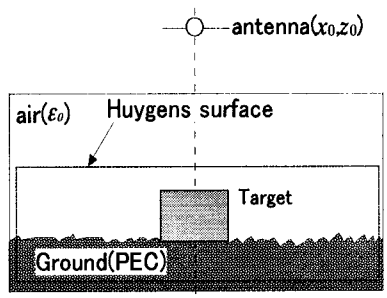

Fig. 4 Schematic of the Huygens surface used to compute the far-zone scattered field.

which use the equivalent electromagnetic current as sources, we can derive the expressions for far field similar to the derivation of expressions for the radiation field of antenna.

2.4 FDTD Analysis

The numerical calculations are implemented by combining the following steps: The radiation field of satellite antenna is derived from Eqs. (1) - (7) and FDTD calculations are carried out using the electromagnetic scattered near field inside the analysis region as initial values, Fig. 3. After the near field of the ground is computed by using FDTD method, Fig. 5, received signal derived from Eqs. (9) - (11).

2.5 Random Surface

The presence of mountains, trees and buildings of various structures lead to random unevenness of the surface of the earth. When the objects on the ground surface are investigated using the reflected radiation, the random uneven ground surface having different material properties becomes an obstacle. Roughness of the ground can be represented using standard deviation of the surface height σ_x and correlation length l.

Next, the autocorrelation function of the surface, and the correlation length which are defined as R(j)=1/e, l=1/e. The rough surface profile is assumed to be of Gaussian random distribution with zero mean-value.

3. Time-Domain Statistical Analysis

By comparing the reflected fields, at identical time, from the flat surface and from the random surface, the error in the received field intensity due to the undesired scattered waves by the random ground surface, can be defined using the following relation.

$$\sigma_{Ey}^2 = \frac{1}{M}\sum_{j=0}^{M-1}\{E_r(j) - E_f(j)\}^2 \quad (12)$$

where, E_r represents the random surface and E_f corresponds to the received signal when the surface is flat. Even if there is a change in the transmission velocity, the detection of ground is still possible as long as the pulse distortion is small. In order to investigate the pulse distorsion due to undesired scattered waves, we

followed a method that employs the correlation coefficient $R_{E_r E_f}$ corresponding to the cases of received signal E_f from the flat surface and received signal E_r from the random surface. The correlation coefficient is given by,

$$R_{E_r,E_k} = \frac{C(E_r,E_f)}{\sigma_{E_r} \cdot \sigma_{E_f}} \tag{13}$$

where,

$$C(E_r,E_f) = \frac{1}{N}\sum_{i=s}^{e}\{E_r(i)-\mu E_r\}\{E_f(i)-\mu E_f\} \tag{14}$$

$$\sigma_{E_f}^2 = \frac{1}{N}\sum_{i=s}^{e}\{E_f(i)-\mu E_f\}^2 \tag{15}$$

$$\sigma_{E_r}^2 = \frac{1}{N}\sum_{i=s}^{e}\{E_r(i)-E_f(i)\}^2 \tag{16}$$

$$\mu E_f = \frac{1}{N}\sum_{i=s}^{e}E_f(i), \quad \mu E_r = \frac{1}{N}\sum_{i=s}^{e}E_r(i).$$

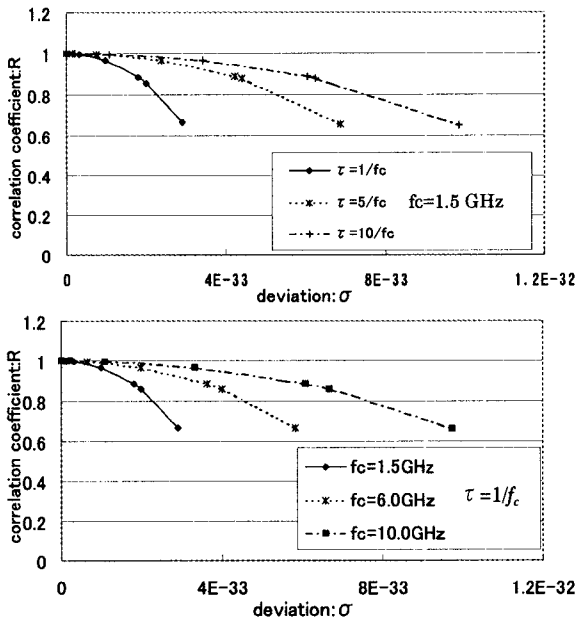

Fig. 5 Correlation length of received signal from random surface (a) mono and multiple pulse widths τ at fc=1.5 GHz (b) various carrier frequencies f_c with the mono pulse width $\tau=1/f_c$.

4. Results and Discussion

4.1 Backscattering Results

In this section, the propagation of radiation field from the antenna is analyzed and we carried out investigations to differentiate the scattering from the object and from the random ground surface. We present numerical examples for various statistical models with random surface characteristics. Fig. 5(a) shows the simulation results on the variaion of correlation coefficient as a function of dispersion for different lenghts of the incident pulse. As observed from the figure, for larger value of pulse length, change in the correlation length is more gradual than the case of short pulse length. The reason for the above observation is due to the fact that the influence of undesired reflected waves from the random ground suface on the received signal is more prominent for the case of smaller pulse length. The above effect is negligible when longer pulse length is used. Similar calculations are carried out for different signal frequencies, and the results are shown in Fig. 5(b). For higher signal frequency, the change in the correlation length is observed to be more gradual than the case of lower frequency. As in the previous case, influence of undesired reflected waves from the random ground suface on the received signal is more prominent at the lower frequency range. From the above statistical analysis, we can obtain the influence of the roughness of random ground surface on received signal at the satellite antenna.

4.2 Backscattering by Object on Random Surface

The standard deviation of the surface of the earth and correlation length for the Case 1 model is shown in Fig. 6(a). t_0=1.893333 msec is the arrival time of pulse front at the ground. Numerical results of the above investigation for two different models are given in Figs.6, 7. The difference in the propagation speed of the scattered fields inside the dielectric objects and air can be observed from the scattering field profiles. This can be better visualized from Fig.6 (d). Because of the difference in propagation speed of the reflected radiation, the wave reflected from the surface of the earth side is observed before the waves reflected from inside of the dielectric object.

Similar electromagnetic scattering analysis was done by varying the parameters as illustrated in Fig. 7. The reflection from ground surface and from the object cannot be distinguished in the received signal, and this is because of the electromagnetic interference occurred above the ground surface. The influence of this electromagnetic interference can be ignored when the standard deviation of surface of the earth side is smaller than pulse length. For the case of larger values of standard deviation, signal processing of received signal is necessary to extract the desired information.

5. Conclusions and Future Directions

We have presented a numerical analysis on the electromagnetic wave scattering for remote sensing applications. We analyzed the signal received at the satellite antenna due to the radiation field from an object located on random ground surface using FDTD method. The difference in the received wave forms for different ground surface conditions is shown. In the future, we planned to repeat similar numerical simulations using more realistic models with more objects on the ground surface and varying angles of signal incidence.

Reference
[1] Y.Miyazaki, K.Takahashi and S.Knedlik: ACES Symposium (1997)
[2] T.Dogaru and L.Carin: IEEE TransA.P., Vol.46, No.3, pp.360-372 (1998)
[3] Y.Miyazaki, K.Takahashi, in Proc. Int. Symp. A.P., Chiba, Japan, (1996)
[4] Y.Miyazaki, J.Sonoda and Y.Jounori: IEE, Vol.117-C-1, pp.35-41, (1997)
[5] K.Takahashi and Y.Miyazaki: IEE, Vol.120-C-1, pp.111-116, (2000)
[6] K.S.Yee: IEEE Trans.A.P., Vol14-3, pp.302-307 (1966)
[7] K.S.Kunz and R.J.Luebbers, Boca Raton, FL: CRC, (1993)
[8] G.Mur: IEEE Trans.EMC., Vol.23-4, pp.377-382, (1981)

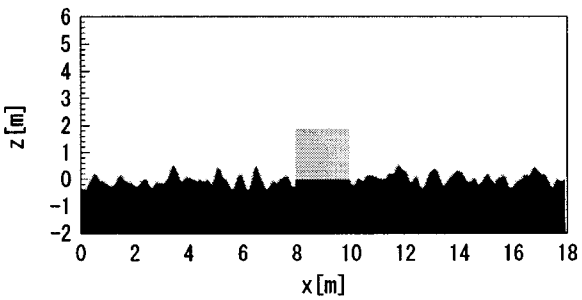

(a)Analysis model

$(\lambda = 0.2m, \sigma_h/\lambda = 1.0, l/\lambda = 1.0)$

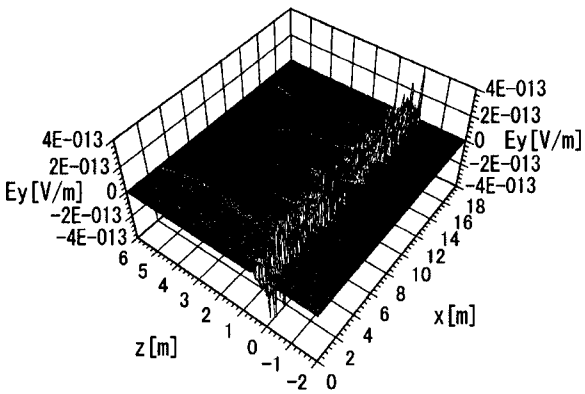

(b)FDTD analysis of near field of surface
($t-t_0$=0.933 nsec)

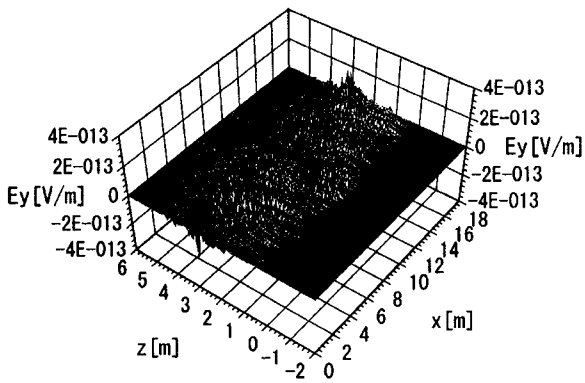

(c)FDTD analysis of near field of surface
($t-t_0$=13.533 nsec)

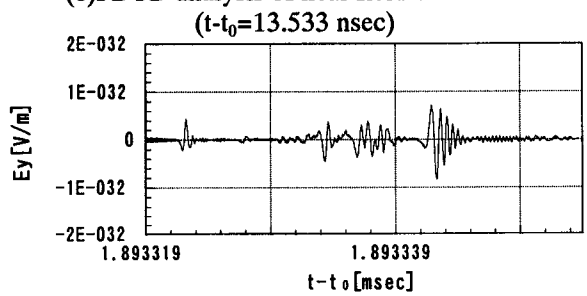

(d) Received signal at satellite antenna

Fig. 6 Analysis models of Case 1, and FDTD results and received signal. t_0=1.893333 msec is the arrival time of pulse front at the ground.

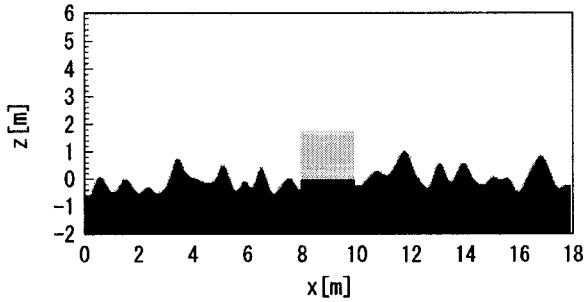

(a)Analysis model

$(\lambda = 0.2m, \sigma_h/\lambda = 2.0, l/\lambda = 2.0)$

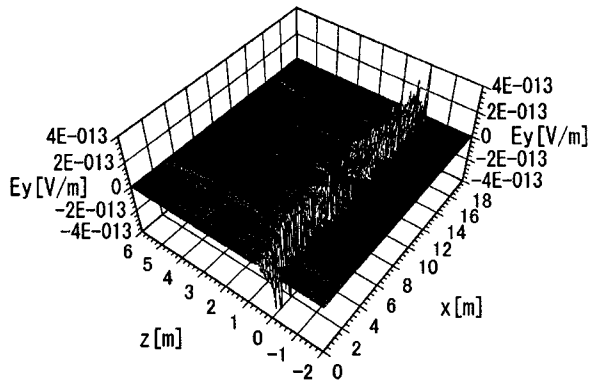

(b)FDTD analysis of near field of surface
($t-t_0$=0.933 nsec)

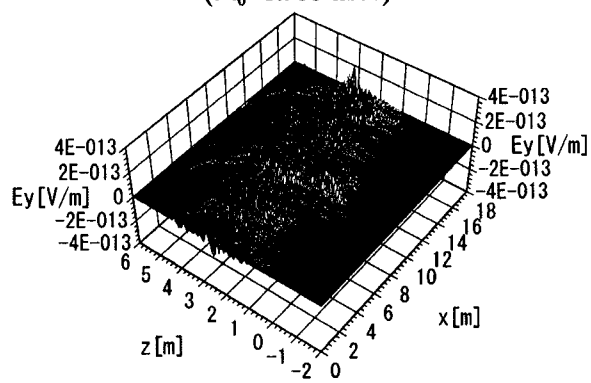

(c)FDTD analysis of near field of surface
($t-t_0$=13.533 nsec)

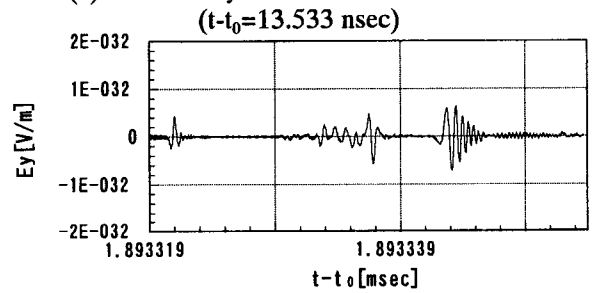

(d) Received signal at satellite antenna

Fig. 7 Analysis models of Case 2 and FDTD results and received signal. t_0=1.893333 msec is the arrival time of pulse front at the ground.